

## Catalytic Hydrolysis of Cellulose to Glucose Using Weak-Acid Surface Sites on Postsynthetically Modified Carbon

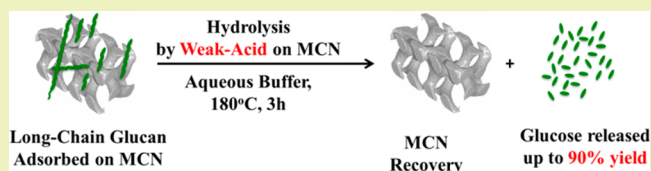
Alexandre Charmot,<sup>†</sup> Po-Wen Chung,<sup>†</sup> and Alexander Katz\*

Department of Chemical and Biomolecular Engineering, University of California, Berkeley, California 94720, United States

## Supporting Information

**ABSTRACT:** We demonstrate depolymerization of adsorbed (1 → 4)- $\beta$ -D-glucans ( $\beta$ -glu) derived from crystalline cellulose (*Avicel*), using weak-acid sites of postsynthetically surface-functionalized mesoporous carbon nanoparticle (MCN) catalysts HT<sub>5</sub>-HSO<sub>3</sub>-MCN and COOH-MCN and investigate the role of acid-site density and  $\beta$ -glu molecular weight on this depolymerization. Both HT<sub>5</sub>-HSO<sub>3</sub>-MCN and COOH-MCN hydrolyze adsorbed  $\beta$ -glu strands and afford glucose yields of 73% and 90%, respectively, at a buffered pH of 2.0 after 3 h treatment at 180 °C. These yields are significantly higher than the 16% yield of an unfunctionalized MCN-control catalyst under otherwise identical conditions, demonstrating the importance of postsynthetic surface functionalization for achieving weak-acid catalytic hydrolysis. Highlighting the important role of confinement in this catalysis, all yields are generally depressed when using a lower rather than higher molecular weight of adsorbed  $\beta$ -glu strands on the same catalyst. The catalytic hydrolysis rate also generally increases upon decreasing buffer pH—particularly so for the more acidic carboxylic acid-functionalized catalyst COOH-MCN. This is interpreted on the basis of a higher local density of surface weak-acid sites upon protonation of surface conjugate-base functionality, as demonstrated by a comparison of zeta potential measurements of catalysts COOH-MCN and MCN.

**KEYWORDS:** Cellulose hydrolysis, Mesoporous carbon, General acid catalysis, Glucan depolymerization, Confinement, Weak acid, OH-Defect site



## INTRODUCTION

The conversion of cellulose, the most abundant form of lignocellulosic biomass on earth, to glucose is generally recognized as a central cost controlling bottleneck for renewable approaches to fuels and chemicals.<sup>1,2</sup> A promising approach that has emerged to overcome this converts recalcitrant crystalline cellulose into dissolved poly(1 → 4)- $\beta$ -D-glucan ( $\beta$ -glu) strands in concentrated acid;<sup>3,4</sup> however, this approach requires costly organic solvents (typically hexanols) for extraction as well as energy inefficiencies during distillation, for the recovery and reuse of concentrated acid.<sup>5,6</sup> An alternative approach is to instead adsorb glucan strands from concentrated acid, thus allowing it to pass through a column and be recycled, followed by release of adsorbed  $\beta$ -glu strands as glucose via depolymerization, which is much more weakly adsorbing.<sup>7</sup> Here, in this manuscript, we demonstrate such a depolymerization using hydrolysis as catalyzed by postsynthetically synthesized weak-acid sites, which due to their mild surface acidity function in the presence of salt prevalent in biomass without leaching acid sites via exchange processes.

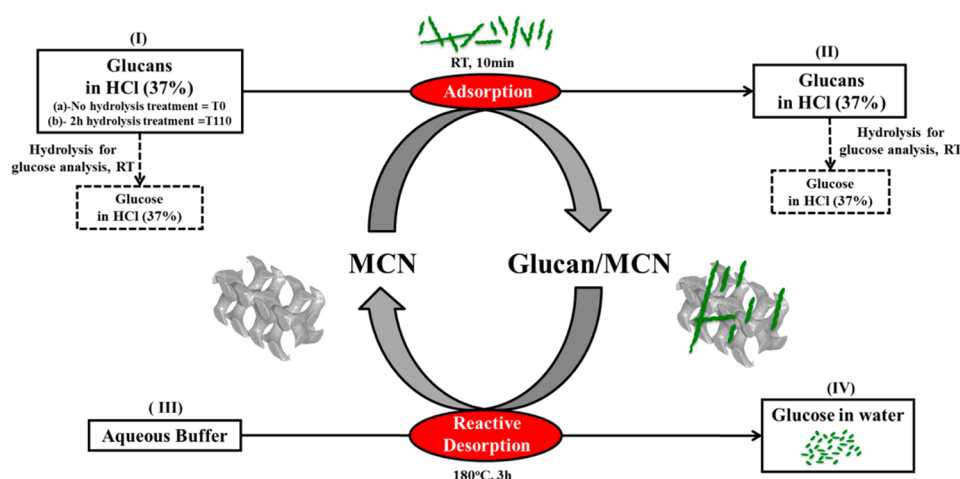
Our approach seamlessly builds on our previous demonstration of catalytic hydrolysis of chemisorbed  $\beta$ -glu strands when using OH-defects as weak-acid sites on inorganic oxide materials, in a manner that was originally inspired by the function of enzymes (cellulases), which consist of a binding and a catalytic domain that consists of weak-acid sites.<sup>8–10</sup> This demonstration laid a detailed blueprint for the design of polysaccharide hydrolysis catalysts consisting of surface weak-

acid sites via postsynthetic surface modification. We showed that essential attributes of this blueprint were a high local density of such sites, as this enforces cooperativity between adsorbed glucans and surface sites via hydrogen-bond formation, and long-chain  $\beta$ -glu confinement and adsorption, which causes glycosidic bonds to be constrained to the proximity of the surface. We demonstrated the latter using mesoporous carbon nanoparticle (MCN) materials, which we showed adsorb long-chain glucans (in excess of 30% by mass),<sup>11</sup> in a process that is driven by CH- $\pi$  interactions and becomes stronger with increasing chain length.<sup>12</sup> This blueprint led us to postsynthetically modify the surface of MCN materials via oxidation treatment, in order to increase the local number density of surface weak-acid OH groups. This postsynthetic modification of MCN led to significantly enhanced catalytic hydrolysis of (1 → 4)- $\beta$ -D-xylans (hemicellulose) derived from *Miscanthus* to xylose, in up to 74% yield under acetate (approximately pH 4) buffered conditions, relative to low yields when using MCN prior to modification instead as catalyst (which resulted in 24% yield). We demonstrated these buffered conditions to lead to inactive catalysts consisting of strong-acid sites such as anchored sulfonic acids, which leach and are neutralized by the buffer salts. We also demonstrated the hydrolytic stability of the weak-acid sites in our being able to recycle catalysts for multiple runs.<sup>13</sup>

Received: October 23, 2014

Published: November 3, 2014

Scheme 1. Schematic of Consecutive Glucan Adsorption from HCl (37 wt %) and Glucan Desorption to Glucose Using MCN as Adsorbents



In this manuscript, we put all of the technical advances described above to task for the depolymerization of cellulose-derived glucan to glucose at the mild pH of a buffered aqueous solution ( $\text{pH} \geq 2.0$ ), by relying on weak-acid surface sites of a MCN-based catalyst. This approach leverages on the catalyst postsynthetic surface-modification procedures and crucially enables a unique comparison of weak-acid hydrolysis catalysis of both hemicellulose and cellulose polysaccharides, as well as the effect of  $\beta$ -glu molecular weight in the case of the latter (vide infra).<sup>13</sup>

The depolymerization of glucans is universally considered to be a more challenging endeavor than for xylans. This is evidenced by the fact that commercial all-synthetic processes (i.e., Quaker Oats and related processes based on acid catalysis at weakly acidic pHs) have existed for the latter for decades,<sup>14</sup> whereas the hydrolysis of the glycosidic bond in cellulose has been thought to require either strong-acid catalysts with  $\text{p}K_a$  below zero or enzymes.<sup>15</sup> In order to depolymerize cellulosic biomass into monosaccharides and other valuable chemicals, carbon materials functionalized with sulfonate groups as strong acid sites have proven valuable<sup>16–18</sup> as well as sulfonated carbon-silica nanocomposites.<sup>19</sup> The exceptions to these have been an emerging literature demonstrating depolymerization of ball-milled cellulose to glucose in high yield (up to 88%) when using various types of unfunctionalized carbon materials as catalyst, which consist of exclusively weak-acid sites on carbon,<sup>20</sup> and depolymerization of cellulose to glucose in water and yields of up to 50% when using graphene-oxide-based catalysts, which also contain only weak-acid sites.<sup>21</sup>

Our approach is unique in that it highlights the benefit of postsynthetically modifying carbon catalysts for  $\beta$ -glu depolymerization with a high local density of weak-acid sites such as surface carboxylic acids and phenolic OH groups. Unlike the case of xylan depolymerization described above, which could be reacted directly from extract solution using excess (relative to adsorption capacity) amounts of xylan, here the material consisting of adsorbed  $\beta$ -glu strands within the MCN pores must be meticulously isolated from the concentrated-acid hydrolyzate before undertaking hydrolysis catalysis. We hypothesized this isolated material to be well-poised for catalytic hydrolysis because the adsorbed  $\beta$ -glu strands are constrained to be proximal to weak-acid sites on the MCN surface and are confined there. This hypothesis is based on the

fact that strain caused by confinement can be relieved via bond breaking of the polysaccharide into shorter segments.<sup>10,22</sup> We investigate the role of confinement on adsorption and catalytic  $\beta$ -glu hydrolysis within the hydrophobic internal 3.2 nm pore diameter of the MCN. This was accomplished by changing the dissolved  $\beta$ -glu molecular weight (by varying the treatment time of  $\beta$ -glu in hydrolyzate solution at room temperature), as measured using GPC.

## EXPERIMENTAL SECTION

**Synthesis of Mesoporous Carbon Nanoparticles (MCN) and Functional Mesoporous Carbon Nanoparticles ( $\text{HT}_n\text{-HSO}_3\text{-MCN}$ ,  $\text{COOH-MCN}$ ).** The synthesis of MCN materials used a MCM-48-type mesoporous silica nanoparticle (MSN) material as the structure-directing template via a modified Stöber approach, as described previously.<sup>23</sup> Afterward surface-functionalized MCN materials were synthesized as described previously.<sup>13</sup> The functional MCN material ( $\text{HSO}_3\text{-MCN}$ ) was synthesized by using fuming  $\text{H}_2\text{SO}_4$  (20% of  $\text{SO}_3$ ) solution as an oxidizing agent. MCN materials (1.2 g) were treated in fuming sulfuric acid solution (80 mL) in a round-bottom flask (50 mL), and the mixture was heated under nitrogen at 80 °C for 24 h. After reaction, the as-synthesized functional MCN were collected via filtration and washed with copious amounts of water. The as-synthesized MCN material (1.2 g) was Soxhlet extracted with 250 mL water for a period of 3 h, and this extraction procedure was repeated four consecutive times. Afterward,  $\text{HSO}_3\text{-MCNs}$  (0.5 g) were placed in an autoclave in the presence of water (15 mL), and hydrothermal treatment was conducted at 200 °C and autogenous pressure for 3 h. The material after the first hydrothermal treatment (denoted as  $\text{HT}_1\text{-HSO}_3\text{-MCN}$ ) was collected by filtration and washed by the aforementioned Soxhlet extraction procedure. Such hydrothermal treatment was repeated for a total of five consecutive times in order to synthesize  $\text{HT}_5\text{-HSO}_3\text{-MCN}$  (and, in general, for a total of  $(n - 1)$  more repetitions in order to synthesize  $\text{HT}_n\text{-HSO}_3\text{-MCN}$ ), as shown in Scheme 1. In order to monitor the sulfate leached out from the carbon surface after the hydrothermal treatment above, 1 mL of  $\text{BaCl}_2$  (1 M) solution was mixed with 1 mL of the filtrate following hydrothermal treatment. Because the solubility product ( $K_{\text{sp}}$ ) of barium sulfate is low ( $1.1 \times 10^{-10}$ ), a white precipitate is observed if there is even trace sulfate (ppb level) present in solution. We observed no white precipitate observed after the fourth hydrothermal treatment. To synthesize  $\text{COOH-MCN}$ , MCNs (300 mg) were placed in a 100 mL round-bottom flask with 30 mL nitric acid (1M), and the solution was refluxed at 105 °C for 1.5 h, filtered hot, washed with copious of water, and Soxhlet extracted in deionized water for 8 h. MCNs and functional MCNs were completely dried under vacuum prior to adsorption and hydrolysis reaction.

**Cellulose Dissolution.** Poly(1 → 4)- $\beta$ -glucan ( $\beta$ -glu) dissolution was achieved by treating crystalline cellulose in concentrated hydrochloric acid (37 wt % aqueous solution) for either (i) a nominally brief time (10 min) that was only enough for dissolution, which is designated here as 0 min glucan hydrolysis at room temperature and leads to Glucan<sub>T0</sub> solution, or (ii) 110 min glucan hydrolysis (i.e., 110 min above and beyond the nominal dissolution time of 10 min) at room temperature, which synthesizes shorter dissolved  $\beta$ -glu strands and is denoted as Glucan<sub>T110</sub> solution. The glucan concentration in the acid hydrolyzate is 2 g glucose eq/L, which is double the value used in previously reported procedures for similar glucan dissolution from cellulose.<sup>11</sup>

**Amorphous  $\beta$ -Glucan.** Amorphous  $\beta$ -glu was reprecipitated as a dry powder from either Glucan<sub>T0</sub> or Glucan<sub>T110</sub> solution in concentrated HCl. In both cases 40 mL of  $\beta$ -glu solution (2 g/L) in HCl (37%) was precipitated by adding this solution to 500 mL of cold acetone (4 °C). The white precipitate thus formed was separated by centrifugation at 4 °C and was washed with cold acetone (4 °C) until a pH of 4 as indicated by pH paper. Then, the white powder was dispersed in water, after final neutralization to pH of 5 (NaOH 1 M solution), and the solution was freeze-dried to obtain a dry white powder of amorphous  $\beta$ -glu.

**Size-Exclusion Chromatography/Gel Permeation Chromatography (SEC/GPC).** For size-exclusion chromatography, approximately 5 mg of dry glucan powder was activated for dissolution by a wetting procedure consisting of a brief continuous wash of water (two times), methanol (two times) and DMAc (two times), followed by dissolution in 8 wt % LiCl/DMAc for 12 h at RT. Following glucan dissolution, the samples were diluted with DMAc so as to produce a 0.5 wt % cellulose in LiCl/DMAc solution, and were subsequently filtered using a 0.2 mm Teflon syringe filter (Whatman). SEC/GPC was performed on a Polymer Laboratories PLGPC-50 instrument, equipped with a refractive index concentration detector (RI). Separation was performed on a two-column series consisting of PLGEL-Mesopore 300 mm × 7.5 mm preceded by a Mesopore guard column 5  $\mu$ M particles 50 mm × 7.5 mm (Polymer Laboratories). The mobile phase consists of 0.5 wt % LiCl in DMAc, and was used at a flow rate of 0.9 mL/min. The oven temperature was set to 50 °C. Calibration data were collected for a series of standards including D-(+)-glucose (Mp = 180), and polysaccharides consisted of the following: stachyose (Mp = 667, Varian) and pullulan polysaccharides (Mp = 5900; 11 100; 21 100; 47 100; 107 000; 200 000; 375 000; 708 000, Varian). The injection volume was set to 100  $\mu$ L, and the run time was set to 75 min. Data acquisition and analysis was performed using Cirrus software.

**Zeta-Potential Measurement.** Zeta potentials of MCN-based materials were measured in a Malvern Zetasizer Nano ZS. Each material was tested in duplicate. Suspensions (100–200  $\mu$ g/mL) of each material in buffer were prepared, and the pH of the buffers was 7.0 (phosphate buffer) and 4.1 (acetate buffer). The zeta potentials were measured immediately after ultrasonication for 1 h.

**Adsorption of  $\beta$ -glu on MCN-Based Catalysts.** Prewighed MCN-based catalyst was treated in a 15 mL polypropylene tube (DB Falcon 352196) with predetermined volumes of concentrated-acid  $\beta$ -glu hydrolyzate solution for 10 min at 4 °C, using a vortex stirrer. Afterward, a SPE column (Phenomenex Strata S-1 Silica, 200 mg/3 mL, 8B-S012-FBJ) separated the solid MCN-based catalyst from filtrate solution. The MCN-based catalyst after filtration was subsequently washed with 3 mL of water in order to remove any traces of concentrated hydrochloric acid, which was monitored using pH strips of the wash solution (pH of final wash correspond to deionized water). After filtration, the solid was dried first by air flow and then overnight under vacuum (0.2 mbar) at room temperature. Only adsorption data representing a significant amount of adsorption via material balance were used and consisted of differences of at least 10% between solutions before and after adsorption.

**Determination of Adsorbed  $\beta$ -glu on MCN-Based Catalyst (HPLC).** The number of glucose equivalents adsorbed on the surface of MCN-based material was determined using a previously described approach,<sup>13</sup> using a Shimadzu HPLC-Refractive Index Detector

equipped with a Biorad Aminex HPX-87H column at 50 °C. Samples were diluted 5-fold prior to analysis and were eluted with a 0.01N H<sub>2</sub>SO<sub>4</sub> mobile phase at a flow rate of 0.6 mL min<sup>-1</sup>. Products were identified by comparison of retention times with corresponding reference compounds. Quantification of the mass concentration of glucose equivalents was determined by the integrated peak area of glucose, using a six-point calibration curve.

**Glucan Depolymerization via Hydrolysis Catalysis and Subsequent Glucose Release.** Typically either 1–2 mg of  $\beta$ -glu or 10–20 mg of dry MCN-based material containing adsorbed  $\beta$ -glu were weighed and placed in a 1.5 mL crimp-top vial, which also contained a stir bar and 1 mL of aqueous buffer solution, at a controlled pH in the range of 2.0–4.6. An acetate buffer (concentration = 0.02 M) was used for pH = 4.6, and phosphate buffer (concentration = 0.02 M) was used for pH = 2.0 and 2.6. The resulting suspension was treated at a constant temperature of 180 °C under 30 rpm stirring, at autogenous pressure, for 3 h. During this time period, hydrolysis occurred, after which the suspension was subsequently cooled to room temperature and transferred to a filtration system. The buffered pH was measured both before and after hydrolysis reaction. A 1 mL SPE column (Burdick and Jackson, 9050, 100 mg/1 mL, Silica) separated solid MCN-based material via filtration, and this material was washed with 2 mL of hot water (80 °C) for completely removing any residual glucose. Glucose and HMF in the wash were analyzed using a Shimadzu HPLC, as described above, except without dilution, which was unnecessary in the absence of HCl.

**Chemicals.** Reagents used for experiments involving high performance liquid chromatography (HPLC) were used as received and were as follows: D-(+)-glucose (99.5%, Sigma), D-(+)-cellobiose (99%, Fluka), HCl (37%, ACS reagent Sigma), H<sub>2</sub>SO<sub>4</sub> (Fluka, solution 5 M), and sodium hydroxide solution (50 wt % in water, Fisher), and HMF (Acros Organics, 98%). Deionized water was obtained from a Milli-Q (18.2 M $\Omega$ ) system by Millipore. Avicel PH101 (11365) was purchased from Fluka Analytical.

## ■ RESULT AND DISCUSSION

We perform a comparative study of three postsynthetically functionalized MCN-based catalysts for the adsorption of  $\beta$ -glu from concentrated acid aqueous solution as well as subsequent depolymerization of these adsorbed  $\beta$ -glu strands, which causes release of soluble glucose, in aqueous buffer media. Our general approach is represented in Scheme 1 and uses the following MCN-based catalysts: (i) MCN—consisting of an unfunctionalized carbon surface with a low density of weak acid sites; (ii) COOH-MCN—consisting of a postsynthetically modified carboxylated carbon surface; and (iii) HT<sub>5</sub>-HSO<sub>3</sub>-MCN—consisting of a postsynthetically modified weak-acid surface that consists mainly of phenolic OH groups.<sup>13</sup> The total density of weak-acid sites on a surface area basis in materials HT<sub>5</sub>-HSO<sub>3</sub>-MCN and COOH-MCN is 2.4- and 2.9-fold higher relative to MCN, respectively (see Supporting Information).

We first investigate  $\beta$ -glu adsorption from concentrated-acid hydrolyzate using two different concentrated-acid aqueous solutions, in order to investigate the effect of glucan-strand molecular weight on adsorption. One of these solutions (Glucan<sub>T0</sub>) was prepared without additional hydrolysis of dissolved crystalline Avicel cellulose in cold concentrated aqueous HCl (37 wt %), whereas the other (Glucan<sub>T110</sub>) underwent a brief hydrolysis consisting of treating this solution for an additional 110 min following dissolution at room temperature. In order to characterize the glucan molecular-weight distribution in these two hydrolyzate solutions, glucans were precipitated via acetone addition, and the molecular weight of  $\beta$ -glu strands was characterized using size-exclusion chromatography (SEC)/GPC. Based on the molecular-weight distribution data in Table 1 and Figure 1, Glucan<sub>T0</sub> solution

**Table 1. Molecular Weight Distribution of (1 → 4)- $\beta$ -Glucan**

	molecular weight of poly(1→4)- $\beta$ -glucan				
	cellobiose repeat	Mp	Mw	Mn	PD <sup>b</sup>
	units <sup>a</sup>	(g/mol)	(g/mol)	(g/mol)	
Glucan <sub>T0</sub>	65	22170	16701	10713	1.56
Glucan <sub>T110</sub>	11	3622	3831	2852	1.34

<sup>a</sup>Numbers of cellobiose repeat units per glucan strand corresponding to Mp in acid hydrolyzate solution. <sup>b</sup>The initial concentration of Glucan<sub>T0</sub> and Glucan<sub>T110</sub> are 2.0 and 2.1 g/L, respectively.

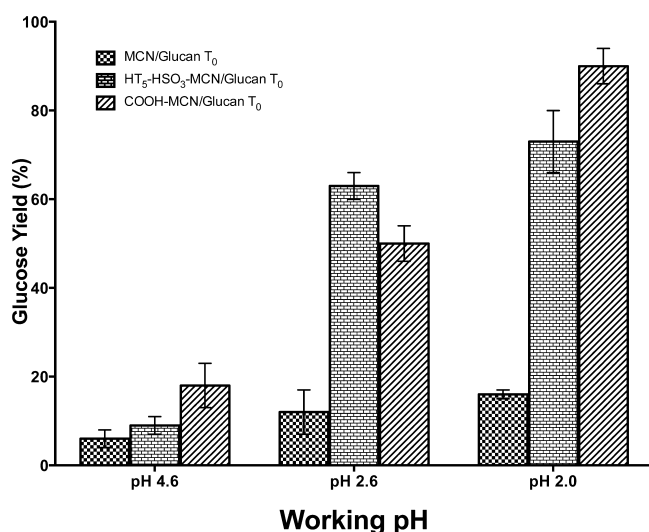


**Figure 1.** Glucose yield using MCN, HT<sub>5</sub>-HSO<sub>3</sub>-MCN, and COOH-MCN materials consisting of adsorbed  $\beta$ -Glu derived from Glucan<sub>T0</sub>. The hydrolysis reaction (3 h, 180 °C) was conducted in sodium phosphate buffer (0.02 M) at pH 2.0 and 2.6 and acetate buffer (0.02M) at pH 4.6.

consists of  $\beta$ -glu strands having a peak-average molecular weight (Mp) of 22 170 g/mol, which corresponds to approximately 65 cellobiose repeating units per glucan chain, and a polydispersity (PD) of 1.56. We also observed a minor peak in the molecular-weight distribution of Glucan<sub>T0</sub>, which is centered at 8000 g/mol. The Glucan<sub>T0</sub>  $\beta$ -glu strands were significantly longer compared with those present in Glucan<sub>T110</sub> solution, which consisted of  $\beta$ -glu strands having a Mp of 3622 g/mol (11 cellobiose repeating units) and a PD of 1.34. This difference represents nearly an order-of-magnitude change in the peak-average molecular weight (factor of 3–4 difference in weight- and number-average molecular weight), due to the additional hydrolysis that occurs during the 110 min period in concentrated HCl aqueous solution at room temperature. Both peak-average molecular weights representing  $\beta$ -glu strands in Glucan<sub>T0</sub> and Glucan<sub>T110</sub> solution have a significantly larger

radius of gyration ( $R_g$ ) in aqueous solution relative to the MCN pore radius,<sup>24</sup> since the molecular-weight cutoff where  $R_g$  of the  $\beta$ -glu strand matches MCN-pore radius occurs at a  $\beta$ -glu molecular weight of 1650.<sup>6</sup> We hypothesize that adsorption, particularly from the longer  $\beta$ -glu strands derived from Glucan<sub>T0</sub> solution, leads to significantly strained  $\beta$ -glu strands. This hypothesis is based in part on the relative curvature of the MCN surface, which we previously reasoned to be on the length scale below a cellotetraose strand, using a comparison of relative free-energies of adsorption of a systematic series of glucose oligomers ranging from glucose to cellotetraose.<sup>11</sup> Such a high curvature of the MCN pore space as well as the confining effects of the pore radius (based on discussion related to  $R_g$  above) are both expected to place significant mechanical strain on adsorbed  $\beta$ -glu strands.

Adsorption data of glucans dissolved in concentrated-acid hydrolyzate solution are summarized in Table 2. These data clearly demonstrate that  $\beta$ -glu strands having a  $R_g$  that is much larger than the pore radius of the MCN adsorb to all three materials, when using both Glucan<sub>T0</sub> and Glucan<sub>T110</sub> solutions (vide supra). Comparing high and low molecular-weight glucan adsorption on HT<sub>5</sub>-HSO<sub>3</sub>-MCN, data in Table 2 show a 1.7-fold higher amount of  $\beta$ -glu adsorption for Glucan<sub>T0</sub> ( $62 \pm 1$  mg Glu equiv/g) relative to Glucan<sub>T110</sub> ( $36 \pm 2$  mg Glu equiv/g). This data shows that  $\beta$ -glu strands of higher molecular weight, which are more prevalent in Glucan<sub>T0</sub> relative to Glucan<sub>T110</sub>, preferentially adsorb onto HT<sub>5</sub>-HSO<sub>3</sub>-MCN. Such an observation is consistent with a previously reported enhanced affinity between the MCN surface and  $\beta$ -glu strand, as the chain length of the latter increases, as driven by cumulative CH- $\pi$  interactions.<sup>11</sup> Yet this does not appear to be general since both high and low molecular weight glucans from Glucan<sub>T0</sub> and Glucan<sub>T110</sub> solutions, respectively, led to similar adsorbed glucan coverages in Table 2 for MCN.

A comparison of COOH-MCN and HT<sub>5</sub>-HSO<sub>3</sub>-MCN in Table 2 shows the effect of surface functionalization on  $\beta$ -glu adsorption. On a surface-area basis, COOH-MCN adsorbed 1.5-fold less  $\beta$ -glu relative to HT<sub>5</sub>-HSO<sub>3</sub>-MCN, under conditions of the adsorption experiment in Table 2, which were performed in a regime where excess adsorbent is present. This may be due to the decreased favorability of forming the required CH- $\pi$  interactions between  $\beta$ -glu strands and surface in COOH-MCN relative to HT<sub>5</sub>-HSO<sub>3</sub>-MCN, as a result of the more polar carboxylated surface in the former. A similar decrease for the more polar COOH-MCN relative to HT<sub>5</sub>-HSO<sub>3</sub>-MCN was not observed for xylans previously.<sup>13</sup> This may be due to the more polar nature of these xylans, which are water soluble, relative to the hydrophobic long-chain glucans investigated here.<sup>13</sup>

We carefully isolated all three materials after adsorption, consisting of  $\beta$ -glu strands on the three MCN-based catalysts,

**Table 2. Adsorption of Glucans with Different Hydrolysis Period onto Functional Mesoporous Carbon Materials**

material consisting of adsorbed $\beta$ -glu strands	hydrolysis time of glucan prior to adsorption <sup>a</sup> (min)	ratio (mg MCN per mL of hydrolyzate)	percentage of $\beta$ -glu adsorbed from the hydrolyzate (%)	[Glu] mg Glu equiv/g of material
MCN/Glucan <sub>T0</sub>	0	4.5	24% $\pm$ 3%	115 $\pm$ 7
HT <sub>5</sub> -SO <sub>3</sub> -MCN/Glucan <sub>T0</sub>	0	11	35% $\pm$ 1%	62 $\pm$ 1
COOH-MCN/Glucan <sub>T0</sub>	0	11	31% $\pm$ 1%	41 $\pm$ 9
MCN/Glucan <sub>T110</sub>	110	4.5	29% $\pm$ 1%	125 $\pm$ 2
HT <sub>5</sub> -SO <sub>3</sub> -MCN/Glucan <sub>T110</sub>	110	11	21% $\pm$ 1%	36 $\pm$ 2

<sup>a</sup>Glucan concentration of 2 g Glu equiv/L, for 10 min at 4 °C.

and investigated catalytic hydrolysis of adsorbed  $\beta$ -glu under buffered pHs of 2.0 (sodium phosphate buffer), 2.6 (sodium phosphate buffer), and 4.6 (sodium acetate buffer) using these isolated materials. We previously demonstrated that such buffered conditions render strong-acid sites such as supported sulfonic acids catalytically inert as their conjugate-base salts.<sup>13</sup> Glucose yields after 3 h at 180 °C are shown in Figures 1 (and Table 3) and 2 (and Table 4) for catalysts consisting of

**Table 3. Reactive Desorption of  $\beta$ -Glu Derived from Glucan<sub>T0</sub> Adsorbed on Carbon Material MCN, HT<sub>5</sub>-SO<sub>3</sub>-MCN, and COOH-MCN at 180 °C for 3 h under Buffered Conditions**

reactive desorption conditions <sup>a</sup>	concentration of glucan on MCN (mg Glu equiv/ gMCN)	initial pH <sup>b</sup>	final pH <sup>c</sup>	glucose yield (%) <sup>d</sup>
MCN/Glucan <sub>T0</sub>	95	4.6	4.0	6%
HT <sub>5</sub> -SO <sub>3</sub> -MCN/ Glucan <sub>T0</sub>	58	4.6	3.9	9%
COOH-MCN/ Glucan <sub>T0</sub>	28	4.6	3.3	18%
MCN/Glucan <sub>T0</sub>	95	2.6	2.5	12%
HT <sub>5</sub> -SO <sub>3</sub> -MCN/ Glucan <sub>T0</sub>	58	2.6	2.5	63%
COOH-MCN/ Glucan <sub>T0</sub>	51	2.6	2.5	50%
MCN/Glucan <sub>T0</sub>	95	2.0	2.0	16%
HT <sub>5</sub> -SO <sub>3</sub> -MCN/ Glucan <sub>T0</sub>	58	2.0	2.0	73%
COOH-MCN/ Glucan <sub>T0</sub>	31	2.0	2.0	90%

<sup>a</sup>Reaction conditions: 1 mL solution, 180 °C, 3 h. <sup>b</sup>pH 4.6 is buffered with [Acetate] = 0.02 M, pH 2.6 and 2.0 are buffered with [PO<sub>4</sub>] = 0.02 M. <sup>c</sup>The final pH is measured after hydrolysis and filtration. <sup>d</sup>Standard deviation is lower than  $\pm 7\%$ .

**Table 4. Reactive Desorption of  $\beta$ -Glu Derived from Glucan<sub>T110</sub> Adsorbed on Carbon Material MCN, HT<sub>5</sub>-SO<sub>3</sub>-MCN at 180 °C for 3 h under Buffered Conditions**

reactive desorption conditions <sup>a</sup>	concentration of glucan on MCN (mg Glu equiv/ gMCN)	initial pH <sup>b</sup>	final pH <sup>c</sup>	glucose yield (%) <sup>d</sup>
MCN/Glucan <sub>T110</sub>	112	4.6	4.0	4%
HT <sub>5</sub> -SO <sub>3</sub> -MCN/ Glucan <sub>T110</sub>	34	4.6	4.1	16%
MCN/Glucan <sub>T110</sub>	112	2.6	2.4	12%
HT <sub>5</sub> -SO <sub>3</sub> -MCN/ Glucan <sub>T110</sub>	34	2.6	2.4	41%
MCN/Glucan <sub>T110</sub>	112	2	2.0	17%
HT <sub>5</sub> -SO <sub>3</sub> -MCN/ Glucan <sub>T110</sub>	34	2	2.0	60%

<sup>a</sup>Reaction conditions: 1 mL solution, 180 °C, 3 h. <sup>b</sup>pH 4.6 is buffered with [acetate] = 0.02 M, pH 2.6 and 2.0 are buffered with [PO<sub>4</sub>] = 0.02 M. <sup>c</sup>The final pH is measured after hydrolysis and filtration. <sup>d</sup>Standard deviation is lower than  $\pm 5\%$ .

adsorbed  $\beta$ -glu strands derived from Glucan<sub>T0</sub> and Glucan<sub>T110</sub>, respectively. In all instances, HMF was only observed as a trace component when glucan was hydrolyzed without MCN and was not detected in any of the experiments involving MCN. Catalyst COOH-MCN hydrolyzed adsorbed  $\beta$ -glu derived from Glucan<sub>T0</sub> in the highest glucose yield of 90% at pH 2.0. This glucose yield is similar to that previously reported in the

hydrolysis of ball-milled cellulose to glucose, in a notable and elegant example of using weak-acid surface sites on a carbon material at pH 2.5 (0.012% aqueous HCl solution).<sup>20</sup> Catalyst HT<sub>5</sub>-HSO<sub>3</sub>-MCN resulted in a slightly lower glucose yield of 73% when using  $\beta$ -glu derived from Glucan<sub>T0</sub> at the same pH. Previous qualitative characterization by infrared spectroscopy demonstrated that HT<sub>5</sub>-HSO<sub>3</sub>-MCN mainly consists of phenolic OH functional groups, whereas catalyst COOH-MCN contains carboxylic-acid surface functionality.<sup>13</sup> The greater glucose yield for HT<sub>5</sub>-HSO<sub>3</sub>-MCN and COOH-MCN over controls consisting of unfunctionalized MCN and buffer background, over all conditions investigated in Tables 3 and 4, demonstrates catalysis by weak-acid sites. This data demonstrates the catalytic benefit of postsynthetic modification of MCN catalyst, which converts it from a highly inactive catalyst to an active one, by increasing the local density of weak-acid sites, according to our original blueprint for catalyst design in this area.<sup>10</sup>

Catalyst COOH-MCN exhibits a greater increase in glucose yield upon lowering the pH, when compared with HT<sub>5</sub>-HSO<sub>3</sub>-MCN. We attribute this greater sensitivity of the COOH-MCN catalyst surface to a decrease in pH as the result of protonation of carboxylic-acid surface functional groups, which appear to be largely absent via ATR-FTIR spectroscopy in catalyst HT<sub>5</sub>-HSO<sub>3</sub>-MCN (vide supra).<sup>13</sup> Such a protonation event at lower pH for carboxylic acid (in COOH-MCN) relative to phenolic (in HT<sub>5</sub>-HSO<sub>3</sub>-MCN) surface functionalities is consistent with the generally greater acidity of the carboxylic-acid functional group (i.e., pK<sub>a</sub> 4.76 for benzoic acid versus pK<sub>a</sub> 10.0 for phenol). We investigated this further by measuring the zeta potential as a relevant measure of residual surface charge as a function of pH for both COOH-MCN and unfunctionalized MCN materials (see the Supporting Information). While the MCN control shows a relatively flat profile in the same pH range, COOH-MCN catalyst exhibits a decreasing surface charge upon decreasing pH, which is consistent with the protonation of carboxylic-acid functional groups. Such a trend in the zeta potential versus pH for COOH-MCN is also consistent with previous observations in related systems consisting of carboxylic-acid monolayers.<sup>25</sup>

A comparison of the effect of adsorbed  $\beta$ -glu molecular weight can also be performed using data in Figures 1 and 2 (or Tables 2 and 3). These data unintuitively demonstrate generally greater glucose yields with Glucan<sub>T0</sub> relative to Glucan<sub>T110</sub>; or, equivalently, it demonstrates that a higher molecular weight adsorbed  $\beta$ -glu strand undergoes depolymerization to glucose much more readily than a smaller strand.<sup>22</sup> This is surprising given the head start that adsorbed  $\beta$ -glu strands derived from Glucan<sub>T110</sub> solution have, as they begin catalytic hydrolysis at the outset already more hydrolyzed (after benefiting from 2 h of hydrolysis in concentrated aqueous HCl at room temperature) when compared with Glucan<sub>T0</sub>. This result suggests that the hydrolysis does not occur in a stepwise fashion in which larger  $\beta$ -glu strands in Glucan<sub>T0</sub> are hydrolyzed to the shorter strands in Glucan<sub>T110</sub>, before hydrolysis to glucose. If this were the case, it would be inconsistent with the former having a higher rate of hydrolysis. Alternatively, this suggests that hydrolysis occurs in a concerted fashion whereby a long-chain  $\beta$ -glu strand is hydrolyzed to either a short oligomer or monomer without going through a slightly shorter chain  $\beta$ -glu strand intermediate. This result also reinforces the significant role of mechanical strain by the confined MCN internal pore space on this process. Such a role of confinement is supported

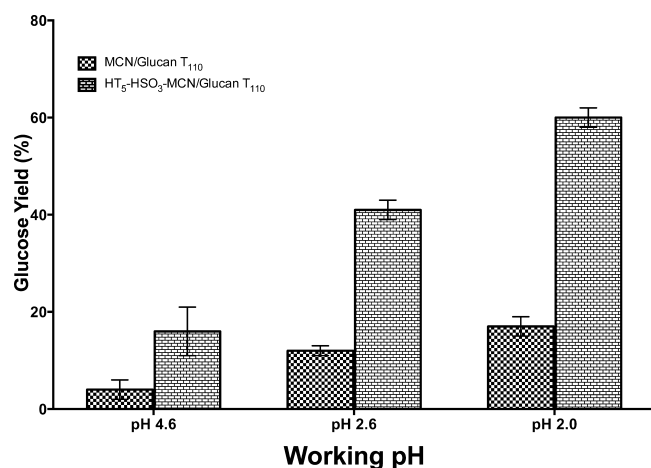


**Figure 2.** Glucose yield using MCN and HT<sub>5</sub>-HSO<sub>3</sub>-MCN materials consisting of adsorbed  $\beta$ -glu derived from Glucan<sub>T110</sub>. The hydrolysis reaction (3 h, 180 °C) was conducted in sodium phosphate buffer (0.02 M) at pH 2.0 and 2.6, and acetate buffer (0.02 M) at pH 4.6.

by recent measurements of the rate constant for catalytic hydrolysis of cellulose to soluble oligomers. This rate constant was measured to be unexpectedly higher than that for soluble oligomers to glucose, in mixed-milling systems consisting of cellulose and carbon catalyst.<sup>22</sup> Thus, the significant role of confinement may be more general and quite possibly applicable in forming soluble oligomers at high rate in the mixed-milling system as well. Previously, during the hydrolysis of (1  $\rightarrow$  4)- $\beta$ -D-xylans using the same MCN-based catalysts, the background hydrolysis rate was similar to the rate observed with MCN catalyst. This led us to conclude in that system that confinement when using MCN catalyst was not enough to differentiate catalytic hydrolysis of xylans over buffer background. The apparent difference in the significance of confinement for the  $\beta$ -glu versus xylan systems may be resolved by considering the much higher molecular weight of polysaccharide strands in the  $\beta$ -glu systems, which is expected to lead to a higher degree of confinement and strain upon adsorption.

HT<sub>5</sub>-HSO<sub>3</sub>-MCN hydrolyzes adsorbed  $\beta$ -glu strands derived from Glucan<sub>T0</sub> solution at pH 2.0 in a 4.6-fold higher glucose yield relative to unfunctionalized MCN. Yet the surface concentration of weak-acid sites in HT<sub>5</sub>-HSO<sub>3</sub>-MCN is only 2.4-fold greater than MCN. This lack of direct correlation between yield and number of sites suggests that not all weak-acid OH sites may be equally active for hydrolysis catalysis—a conclusion shared previously for catalytic hydrolysis of xylans in solution.<sup>13</sup> From this perspective, we hypothesize that the active sites responsible for observed hydrolysis catalysis consist of that fraction of weak-acid sites that is expressed in a high local density of the carbon surface, which may be present in either defect-site pockets or nests. This would be consistent with our previous studies involving hydrolysis of adsorbed  $\beta$ -glu strands using weak-acid OH-defect sites on inorganic-oxide surfaces, which directly correlate local density of these sites to the  $\beta$ -glu hydrolysis catalytic activity.<sup>10</sup>

In summary, postsynthetically surface-functionalized MCN-based materials readily adsorb  $\beta$ -glu strands derived from *Avicel*, when using concentrated acid as solvent. These materials catalyze the depolymerization of adsorbed  $\beta$ -glu strands via glycosidic bond hydrolysis in glucose yields of up to 90% at a buffered pH of 2.0, after treatment at 180 °C for 3 h.

Comparisons with unfunctionalized MCN reaction under similar conditions highlight the role of weak-acid sites that are present in high local density on the surface as the catalytically relevant sites, whereas comparisons between adsorbed glucans of varying molecular weight highlights the positive benefit of confinement on depolymerization. When combined together with our previous demonstration of xylan adsorption and polymerization,<sup>13</sup> the results contained in this manuscript demonstrate catalysts consisting of postsynthetically functionalized carbon and composed of weak-acid sites can be used for depolymerizing the carbohydrate component of biomass, consisting of hemicellulose and cellulose, which makes up the majority component and fermentable fraction of lignocellulosic biomass. These MCN-based catalysts combine crucial elements of enzymes including cumulative weak CH- $\pi$  interactions with polysaccharide chains so as to cause adsorption,<sup>26,27</sup> confinement so as to cause ensuing mechanical strain of the adsorbed strand,<sup>28–32</sup> as well as a weak-acid site for catalyzing hydrolysis.<sup>33,34</sup>

## ■ ASSOCIATED CONTENT

### 📄 Supporting Information

(1) GPC traces characterizing Glucan<sub>T0</sub> and Glucan<sub>T110</sub>. (2) Surface properties of MCN-based catalysts. (3) Zeta potential measurements of MCN, COOH-MCN at pH 7 and 4.1. (4) Reactor setup used for performing the hydrolysis reaction. This material is available free of charge via the Internet at <http://pubs.acs.org>.

## ■ AUTHOR INFORMATION

### ✉ Corresponding Author

\*E-mail: [katz@cchem.berkeley.edu](mailto:katz@cchem.berkeley.edu).

### ✎ Author Contributions

†A.C. and P.-W.C. contributed equally to this work.

### 📌 Notes

The authors declare no competing financial interest.

## ■ ACKNOWLEDGMENTS

This work was supported by the Energy Bioscience Institute.

## ■ REFERENCES

- (1) Lam, E.; Luong, J. H. T. Carbon materials as catalyst supports and catalysts in the transformation of biomass to fuels and chemicals. *ACS Catal.* **2014**, *4* (10), 3393–3410.
- (2) Wyman, E. C. Biomass Ethanol: Technical progress, opportunities, and commercial challenges. *Annu. Rev. Energy Environ.* **1999**, *24*, 189–226.
- (3) Wang, H.; Gurau, G.; Rogers, R. D. Ionic liquid processing of cellulose. *Chem. Soc. Rev.* **2012**, *41* (4), 1519–1537.
- (4) Luterbacher, J. S.; Rand, J. M.; Alonso, D. M.; Han, J.; Youngquist, J. T.; Maravelias, C. T.; Pfleger, B. F.; Dumesic, J. A. Nonenzymatic sugar production from biomass using biomass-derived  $\gamma$ -valerolactone. *Science* **2014**, *17*, 277–280.
- (5) Forster, V.; Martz, L. E.; Leng, D. E. Process for recovering concentrated hydrochloric acid from crude product obtained from acid hydrolysis of cellulose. EP0018621A1, November 12, 1980.
- (6) Jansen, R.; Eyal, A. Systems and methods for sugar refining. WO2012106727A1, August 9, 2012.
- (7) Chung, P. W.; Charmot, A.; Katz, A.; Gokhale, A. A. Carbonaceous material for purifying lignocellulosic oligomers. CA2850993A1, April 25, 2013.
- (8) Gazit, O. M.; Charmot, A.; Katz, A. Grafted cellulose strands on the surface of silica: effect of environment on reactivity. *Chem. Commun.* **2011**, *47*, 376–378.

- (9) Gazit, O. M.; Katz, A. Grafted poly(1→4- $\beta$ -glucan) strands on silica: A comparative study of surface reactivity as a function of grafting density. *Langmuir* **2011**, *28* (1), 431–437.
- (10) Gazit, O. M.; Katz, A. Understanding the role of defect sites in glucan hydrolysis on surfaces. *J. Am. Chem. Soc.* **2013**, *135* (11), 4398–4402.
- (11) Chung, P.-W.; Charmot, A.; Gazit, O. M.; Katz, A. Glucan adsorption on mesoporous carbon nanoparticles: Effect of chain length and internal surface. *Langmuir* **2012**, *28* (43), 15222–15232.
- (12) Yabushita, M.; Kobayashi, H.; Hasegawa, J.-y.; Hara, K.; Fukuoka, A. Entropically favored adsorption of cellulosic molecules onto carbon materials through hydrophobic functionalities. *ChemSusChem* **2014**, *7* (5), 1443–1450.
- (13) Chung, P.-W.; Charmot, A.; Olatunji-Ojo, O. A.; Durkin, K. A.; Katz, A. Hydrolysis catalysis of Miscanthus xylan to xylose using weak-acid surface sites. *ACS Catal.* **2013**, *4* (1), 302–310.
- (14) Zeitsch, K. J. *The chemistry and technology of furfural and its many by-products*; Elsevier: Amsterdam, 2000.
- (15) Rinaldi, R.; Meine, N.; vom Stein, J.; Palkovits, R.; Schüth, F. Which controls the depolymerization of cellulose in ionic liquids: The solid acid catalyst or cellulose? *ChemSusChem* **2010**, *3* (2), 266–276.
- (16) Onda, A.; Ochi, T.; Yanagisawa, K. Selective hydrolysis of cellulose into glucose over solid acid catalysts. *Green Chem.* **2008**, *10* (10), 1033–1037.
- (17) Pang, J.; Wang, A.; Zheng, M.; Zhang, T. Hydrolysis of cellulose into glucose over carbons sulfonated at elevated temperatures. *Chem. Commun.* **2010**, *46* (37), 6935–6937.
- (18) Suganuma, S.; Nakajima, K.; Kitano, M.; Yamaguchi, D.; Kato, H.; Hayashi, S.; Hara, M. Hydrolysis of cellulose by amorphous carbon bearing SO<sub>3</sub>H, COOH, and OH groups. *J. Am. Chem. Soc.* **2008**, *130* (38), 12787–12793.
- (19) Van de Vyver, S.; Peng, L.; Geboers, J.; Schepers, H.; de, C. F.; Gommers, C. J.; Goderis, B.; Jacobs, P. A.; Sels, B. F. Sulfonated silica/carbon nanocomposites as novel catalysts for hydrolysis of cellulose to glucose. *Green Chem.* **2010**, *12*, 1560–1563.
- (20) Kobayashi, H.; Yabushita, M.; Komanoya, T.; Hara, K.; Fujita, I.; Fukuoka, A. High-yielding one-pot synthesis of glucose from cellulose using simple activated carbons and trace hydrochloric acid. *ACS Catal.* **2013**, *3* (4), 581–587.
- (21) Zhao, X.; Wang, J.; Chen, C.; Huang, Y.; Wang, A.; Zhang, T. Graphene oxide for cellulose hydrolysis: how it works as a highly active catalyst? *Chem. Commun.* **2014**, *50* (26), 3439–3442.
- (22) Yabushita, M.; Kobayashi, H.; Hara, K.; Fukuoka, A. Quantitative evaluation of ball-milling effects on the hydrolysis of cellulose catalysed by activated carbon. *Catal. Sci. Technol.* **2014**, *4* (8), 2312–2317.
- (23) Kim, T.-W.; Chung, P.-W.; Slowing, I. I.; Tsunoda, M.; Yeung, E. S.; Lin, V. S. Y. Structurally ordered mesoporous carbon nanoparticles as transmembrane delivery vehicle in human cancer cells. *Nano Lett.* **2008**, *8* (11), 3724–3727.
- (24) Dumitriu, S. *Polysaccharides: Structural diversity and functional versatility*; CRC Press: Boca Raton, 2005.
- (25) Shyue, J.-J.; De Guire, M. R.; Nakanishi, T.; Masuda, Y.; Koumoto, K.; Sukenik, C. N. Acid–base properties and zeta potentials of self-assembled monolayers obtained via in situ transformations. *Langmuir* **2004**, *20* (20), 8693–8698.
- (26) Kiehna, S. E.; Laughrey, Z. R.; Waters, M. L. Evaluation of a carbohydrate- $\pi$  interaction in a peptide model system. *Chem. Commun.* **2007**, *39*, 4026–4028.
- (27) Payne, C. M.; Bomble, Y. J.; Taylor, C. B.; McCabe, C.; Himmel, M. E.; Crowley, M. F.; Beckham, G. T. Multiple functions of aromatic-carbohydrate interactions in a processive cellulase examined with molecular simulation. *J. Biol. Chem.* **2011**, *286* (47), 41028–41035.
- (28) Saharay, M.; Guo, H.; Smith, J. C. Catalytic mechanism of cellulose degradation by a cellobiohydrolase, CelS. *PLoS One* **2010**, *5*, e12947.
- (29) Davies, G. J.; Mackenzie, L.; Varrot, A.; Dauter, M.; Brzozowski, A. M.; Schülein, M.; Withers, S. G. Snapshots along an enzymatic reaction coordinate: Analysis of a retaining  $\beta$ -glycoside hydrolase. *Biochemistry* **1998**, *37* (34), 11707–11713.
- (30) Hrmova, M.; Fincher, G. B. Dissecting the catalytic mechanism of a plant  $\beta$ -d-glucan glucohydrolase through structural biology using inhibitors and substrate analogues. *Carbohydr. Res.* **2007**, *342* (12–13), 1613–1623.
- (31) Brameld, K. A.; Goddard, W. A. Substrate distortion to a boat conformation at subsite –1 is critical in the mechanism of family 18 chitinases. *J. Am. Chem. Soc.* **1998**, *120* (15), 3571–3580.
- (32) Petersen, L.; Ardèvol, A.; Rovira, C.; Reilly, P. J. Mechanism of cellulose hydrolysis by inverting GH8 endoglucanases: A QM/MM metadynamics study. *J. Phys. Chem. B* **2009**, *113* (20), 7331–7339.
- (33) Capon, B. Intramolecular catalysis in glucoside hydrolysis. *Tetrahedron Lett.* **1963**, 911–13.
- (34) Capon, B. Mechanism in carbohydrate chemistry. *Chem. Rev.* **1969**, *69*, 407–98.